

Finite Element Based Initial Post-buckling Analysis of Conical Shell Structures

T. Rahman¹, E. L. Jansen¹ and J. J. Wijker²

¹Delft University of Technology, Faculty of Aerospace Engineering
Kluyverweg 1, 2629 HS Delft
The Netherlands

²Dutch Space BV
Newtonweg 1, 2333 CP Leiden
The Netherlands

Keywords: Post-buckling, Conical shells, Finite elements, Perturbation method

ABSTRACT

In this paper a finite element implementation of Koiter's initial post-buckling theory is presented. In the present implementation the effect of pre-buckling nonlinearity has been taken into account. Using this implementation a reduced complexity analysis has been done of the conical interstage of the Vega Launcher, idealized as a conical shell. The general purpose finite element software DIANA has been used as the development platform. Results are compared with a semi-analytical analysis.

1 INTRODUCTION

Thin-walled cylindrical and conical shells are the main structural components in space industry for spacecraft and launch vehicles. Buckling is the key design criterion for these thin-walled structures. Moreover, this type of structures exhibit unstable post-buckling behavior which make them highly sensitive to small geometric or load imperfections. Standard finite element based incremental-iterative analysis approach of such structures is computationally expensive and not suitable for repeated runs necessary for a design and optimization process, and often it is difficult to interpret the result and guarantee its correctness. Hence there is a strong need for intermediate tools that address the aforementioned shortcomings. In the present work a modified form of Koiter's perturbation approach proposed by Byskov and Hutchinson [1] is used as the foundation of such intermediate tools. In this approach a perturbation expansion of the initial post-buckling displacement field is made in terms

of buckling modes and corresponding second order modes. Often a limited number of modes are sufficient and consequently the initial post-buckling behaviour can be described by a small set of nonlinear algebraic equations (the number of equations are the same as the number of buckling modes chosen). In this paper we will present a single mode analysis. Along with the computation of buckling and second order modes the post-buckling slope (a coefficient) and curvature (b coefficient) are also computed. These post-buckling coefficients give a measure of the stability and imperfection sensitivity of the structure. For instance in the case of conical and cylindrical shells we have zero a coefficients and typically negative b coefficients indicating unstable post-buckling behavior with high imperfection sensitivity. It is to be noted that the present paper is concerned with static analysis. The perturbation approach can also be applied to dynamic analysis [2], [3].

The theory of initial post-buckling behavior as developed by Koiter [4] is a perturbation technique based on the principle of stationary potential energy. However in this paper we will follow an alternate procedure, proposed by Budiansky and Hutchinson [1] that writes the field equations directly in variational form using the principle of virtual work. In Budiansky and Hutchinson's work the pre-buckling state was assumed linear. In the present work we analyse the idealized conical interstage of the Vega Launcher [5] under axial compression where it is important to account for the pre-buckling nonlinearity. In fact for this particular problem it is not possible to determine

the first buckling mode correctly if the pre-buckling nonlinearity is ignored. Cohen [6] and Fitch [7] and later Arbocz and Hol [8, 9] derived the modifications triggered by the pre-buckling nonlinearity. These modifications have been included in the present implementation which has been done in the development environment of the general purpose finite element software DIANA [10]. The implementation is largely based on DIANA's existing implementation and Tiso's formulation [11].

2 THE PERTURBATION METHOD

In this section we will discuss the perturbation method for buckling and post-buckling analysis with the inclusion of pre-buckling nonlinearity. Detailed derivation of the equations are available in the report by Arbocz and Hol [9]. Here we will explain the basic procedure and mention the essential equations. The functional notation introduced by Budiansky [12] will be used. In the following, symbols with bold font denote vector and tensor quantities while the scalar symbols are written in normal font.

Let us define \mathbf{u} , $\boldsymbol{\epsilon}$, \mathbf{f} and $\boldsymbol{\sigma}$ as the generalized displacement, strain, load and stress variables. Then the nonlinear strain-displacement relation (1) and the linear elastic constitutive relation (2) can be written as

$$(1) \quad \boldsymbol{\epsilon} = L_1(\mathbf{u}) + \frac{1}{2}L_2(\mathbf{u})$$

$$(2) \quad \boldsymbol{\sigma} = H(\boldsymbol{\epsilon})$$

where L_1 and H are linear functionals and L_2 is a quadratic functional. The equilibrium equation in variational form is written as

$$(3) \quad \boldsymbol{\sigma} \cdot \delta \boldsymbol{\epsilon} - \mathbf{f} \cdot \delta \mathbf{u} = 0$$

Here $\boldsymbol{\sigma} \cdot \delta \boldsymbol{\epsilon}$ and $\mathbf{f} \cdot \delta \mathbf{u}$ denote, respectively, the internal virtual work of the stress $\boldsymbol{\sigma}$ through the strain variation $\delta \boldsymbol{\epsilon}$, and the external virtual work of the load \mathbf{f} through the displacement variation $\delta \mathbf{u}$, both integrated over the entire structure. Further if the bilinear functional L_{11} is defined such that

$$(4) \quad L_2(\mathbf{u} + \mathbf{v}) = L_2(\mathbf{u}) + 2L_{11}(\mathbf{u}, \mathbf{v}) + L_2(\mathbf{v})$$

then it follows from (1) that the first order strain variation $\delta \boldsymbol{\epsilon}$ produced by $\delta \mathbf{u}$ can be written as

$$(5) \quad \delta \boldsymbol{\epsilon} = L_1(\delta \mathbf{u}) + L_{11}(\mathbf{u}, \delta \mathbf{u})$$

We also assume that the reciprocity relation

$$(6) \quad \boldsymbol{\sigma}_i \cdot \boldsymbol{\epsilon}_j = \boldsymbol{\sigma}_j \cdot \boldsymbol{\epsilon}_i \quad (i, j = 1, 2 \dots)$$

holds. In this study we consider proportional loading, i.e. $\mathbf{f} = \lambda \mathbf{f}_0$. Now the variables $(\mathbf{u}, \boldsymbol{\epsilon}, \boldsymbol{\sigma})$ of the post-buckling equilibrium state can be expanded in the following perturbation series about the pre-buckling equilibrium state $(\mathbf{u}_0, \boldsymbol{\epsilon}_0, \boldsymbol{\sigma}_0)$ at the same value of the variable load parameter λ

$$(7) \quad \begin{aligned} \mathbf{u} &= \mathbf{u}_0 + \mathbf{u}_1 \xi + \mathbf{u}_2 \xi^2 + \mathbf{u}_3 \xi^3 + \dots \\ \boldsymbol{\epsilon} &= \boldsymbol{\epsilon}_0 + \boldsymbol{\epsilon}_1 \xi + \boldsymbol{\epsilon}_2 \xi^2 + \boldsymbol{\epsilon}_3 \xi^3 + \dots \\ \boldsymbol{\sigma} &= \boldsymbol{\sigma}_0 + \boldsymbol{\sigma}_1 \xi + \boldsymbol{\sigma}_2 \xi^2 + \boldsymbol{\sigma}_3 \xi^3 + \dots \end{aligned}$$

The variables $(\mathbf{u}_0, \boldsymbol{\epsilon}_0, \boldsymbol{\sigma}_0)$ and $(\mathbf{u}, \boldsymbol{\epsilon}, \boldsymbol{\sigma})$ are assumed to be nonlinear functions of $\lambda = \lambda(\xi)$, while the expansion functions $(\mathbf{u}_k, \boldsymbol{\epsilon}_k, \boldsymbol{\sigma}_k)$ where $k = 1, 2, \dots$ are independent of λ and ξ . The perturbation expansions (7) are assumed to be asymptotically valid in the neighbourhood of the critical point defined by $\lambda = \lambda_c$ and $\xi = 0$.

Substituting equations (7) into equations (1), (2) and (3), taking the limit $\xi \rightarrow 0$ and with some further manipulations one obtains the necessary equations for the buckling load λ_c and the corresponding buckling mode \mathbf{u}_1

$$(8) \quad \boldsymbol{\epsilon}_1 = L_1(\mathbf{u}_1) + L_{11}(\mathbf{u}_c, \mathbf{u}_1)$$

$$(9) \quad \boldsymbol{\sigma}_1 = H(\boldsymbol{\epsilon}_1)$$

$$(10) \quad \boldsymbol{\sigma}_1 \cdot \delta \boldsymbol{\epsilon}_c + \boldsymbol{\sigma}_c \cdot L_{11}(\mathbf{u}_1, \delta \mathbf{u}) = 0$$

where the pre-buckling quantities with the subscript $(\)_c$ are evaluated at $\lambda = \lambda_c$. Next it is assumed that the pre-buckling variables can be expanded in the Taylor series

$$(11) \quad \begin{aligned} \mathbf{u}_0 &= \mathbf{u}_c + (\lambda - \lambda_c) \dot{\mathbf{u}}_c \\ &\quad + \frac{1}{2}(\lambda - \lambda_c)^2 \ddot{\mathbf{u}}_c + \dots \\ \boldsymbol{\sigma}_0 &= \boldsymbol{\sigma}_c + (\lambda - \lambda_c) \dot{\boldsymbol{\sigma}}_c \\ &\quad + \frac{1}{2}(\lambda - \lambda_c)^2 \ddot{\boldsymbol{\sigma}}_c + \dots \end{aligned}$$

where the dots represent differentiation with respect to λ . In addition it will be assumed that $(\lambda - \lambda_c)$ admits the asymptotic perturbation expansion

$$(12) \quad \lambda - \lambda_c = a \lambda_c \xi + b \lambda_c \xi^2 + \dots$$

In view of equation (12), if a plot of load parameter (λ) versus the mode amplitude (ξ) is made then a and b coefficients respectively indicate the slope

and curvature of the post-buckling curve. In the present work we consider symmetric structures with post-buckling slope, $a = 0$ and typically negative post-buckling curvature, $b < 0$ indicating unstable post-buckling behavior.

Inserting equations (11) and (12) together with equation (7) into equations (1), (2) and (3) and equating the coefficients of ξ^2 with the assumption of $a = 0$ (valid for symmetric structures) one can finally obtain the necessary equations for the determination of the second order mode \mathbf{u}_2

$$(13) \quad \epsilon_2 = L_1(\mathbf{u}_2) + L_{11}(\mathbf{u}_c, \mathbf{u}_2) + \frac{1}{2}L_2(\mathbf{u}_1)$$

$$(14) \quad \boldsymbol{\sigma}_2 = H(\epsilon_2)$$

$$(15) \quad \boldsymbol{\sigma}_2 \cdot \delta \epsilon_c + \boldsymbol{\sigma}_c \cdot L_{11}(\mathbf{u}_2, \delta \mathbf{u}) + \boldsymbol{\sigma}_1 \cdot L_{11}(\mathbf{u}_1, \delta \mathbf{u}) = 0$$

The second order mode \mathbf{u}_2 is further subject to the following orthogonality condition

$$(16) \quad \boldsymbol{\sigma}_c \cdot L_{11}(\mathbf{u}_1, \mathbf{u}_2) = 0$$

In order to obtain the expression for the b coefficient we set $\delta \mathbf{u} = \mathbf{u}_1$ in equations (10) and (15) and make use of the reciprocity relation (6). This gives

$$(17) \quad b = -\frac{2\boldsymbol{\sigma}_1 \cdot L_{11}(\mathbf{u}_1, \mathbf{u}_2) + \boldsymbol{\sigma}_2 \cdot L_2(\mathbf{u}_1)}{\lambda_c \hat{\lambda}}$$

where

$$(18) \quad \hat{\lambda} = 2\boldsymbol{\sigma}_1 \cdot L_{11}(\dot{\mathbf{u}}_c, \mathbf{u}_1) + \dot{\boldsymbol{\sigma}}_c \cdot L_2(\mathbf{u}_1)$$

3 FINITE ELEMENT IMPLEMENTATION

In this section we will discuss the finite element implementation of the perturbation approach described in the section 2. An existing DIANA element called CQ40S has been used. CQ40S is an eight-node quadrilateral iso-parametric curved shell element. At each node it has 3 displacement degrees of freedom and 2 rotational degrees of freedom. Therefore the element has 5 degrees of freedom per node leading to 40 (5×8) degrees of freedom for the whole element. It is based on Mindlin's shell theory and both displacements and rotations are interpolated independently using quadratic polynomials. To avoid membrane and shear locking a reduced integration 2×2 scheme is used over the element area. Integration in thickness direction can be 3 point Simpson or 2 point Gauss. Details of this element is available in DIANA manual [10]. Here only the relevant parts concerning buckling and post-buckling analysis are described. We use bold font to denote vectors and matrices and normal font for scalars.

In order to use the element CQ40S for post-buckling analysis no modification of the element formulation is required. However it is necessary to construct the non-linear part of strain-displacement matrix named as \mathbf{B}_{NL} . In FE notation the strain-displacement relation is given as

$$(19) \quad \boldsymbol{\epsilon} = \mathbf{B}_L \mathbf{q} + \frac{1}{2} \mathbf{B}_{NL} \mathbf{q}$$

where \mathbf{B}_L and \mathbf{B}_{NL} defined at each integration point correspond respectively to L_1 and L_2 functionals in equation (1) and \mathbf{q} is the vector of nodal displacements at each element corresponding to continuous displacement field (\mathbf{u}). Equation (19) is written in terms of Green-Lagrange strain tensor as

$$(20) \quad \begin{bmatrix} \epsilon_{xx} \\ \epsilon_{yy} \\ \epsilon_{zz} \\ \epsilon_{xy} \\ \epsilon_{yz} \\ \epsilon_{zx} \end{bmatrix} = \underbrace{\begin{bmatrix} u_{x,x} \\ u_{y,y} \\ u_{z,z} \\ \frac{1}{2}(u_{x,y} + u_{y,x}) \\ \frac{1}{2}(u_{y,z} + u_{z,y}) \\ \frac{1}{2}(u_{z,x} + u_{x,z}) \end{bmatrix}}_{\mathbf{B}_L \mathbf{q}} + \frac{1}{2} \underbrace{\begin{bmatrix} u_{x,x}^2 + u_{y,x}^2 + u_{z,x}^2 \\ u_{x,y}^2 + u_{y,y}^2 + u_{z,y}^2 \\ u_{x,z}^2 + u_{y,z}^2 + u_{z,z}^2 \\ u_{x,x}u_{x,y} + u_{y,x}u_{y,y} + u_{z,x}u_{z,y} \\ u_{x,y}u_{x,z} + u_{y,y}u_{y,z} + u_{z,y}u_{z,z} \\ u_{x,z}u_{x,x} + u_{y,z}u_{y,x} + u_{z,z}u_{z,x} \end{bmatrix}}_{\mathbf{B}_{NL}(\mathbf{q})\mathbf{q}}$$

where ϵ_{xx} , ϵ_{yy} , ϵ_{zz} , ϵ_{xy} , ϵ_{yz} and ϵ_{zx} are the strain components and u_x , u_y and u_z are the displacement components. It is to be noted that unlike \mathbf{B}_L , \mathbf{B}_{NL} is a function of \mathbf{q} since it gives the nonlinear part of the strain. Finally \mathbf{B}_{NL} is constructed as

$$(21) \quad \mathbf{B}_{NL}(\mathbf{q}) = \begin{bmatrix} \mathbf{q}^T \mathbf{K}_{xx} \\ \mathbf{q}^T \mathbf{K}_{yy} \\ \mathbf{q}^T \mathbf{K}_{zz} \\ \mathbf{q}^T \mathbf{K}_{xy} \\ \mathbf{q}^T \mathbf{K}_{yz} \\ \mathbf{q}^T \mathbf{K}_{zx} \end{bmatrix}$$

where the matrices \mathbf{K}_{xx} , \mathbf{K}_{yy} , \mathbf{K}_{zz} , \mathbf{K}_{xy} , \mathbf{K}_{yz} , \mathbf{K}_{zx} are defined as

$$(22) \quad \begin{aligned} \mathbf{K}_{xx} &= \mathbf{N}_{,x}^T \mathbf{N}_{,x} \\ \mathbf{K}_{yy} &= \mathbf{N}_{,y}^T \mathbf{N}_{,y} \\ \mathbf{K}_{zz} &= \mathbf{N}_{,z}^T \mathbf{N}_{,z} \\ \mathbf{K}_{xy} &= \frac{1}{2}(\mathbf{N}_{,x}^T \mathbf{N}_{,y} + \mathbf{N}_{,y}^T \mathbf{N}_{,x}) \\ \mathbf{K}_{yz} &= \frac{1}{2}(\mathbf{N}_{,y}^T \mathbf{N}_{,z} + \mathbf{N}_{,z}^T \mathbf{N}_{,y}) \\ \mathbf{K}_{zx} &= \frac{1}{2}(\mathbf{N}_{,z}^T \mathbf{N}_{,x} + \mathbf{N}_{,x}^T \mathbf{N}_{,z}) \end{aligned}$$

Here $\mathbf{N}_{,x}$, $\mathbf{N}_{,y}$, $\mathbf{N}_{,z}$ are the derivatives of the interpolation polynomial functions at each integration point of the element. Thus the functional $L_2(\mathbf{u})$ is represented by $\mathbf{B}_{NL}(\mathbf{q})$ and in a similar way $L_{11}(\mathbf{u}, \mathbf{v})$ is translated to finite element notation as $\mathbf{B}_{NL}(\mathbf{q}_1)\mathbf{q}_2$ where the nodal displacement vectors \mathbf{q}_1 and \mathbf{q}_2 correspond to continuous displacement fields \mathbf{u} and \mathbf{v} respectively.

3.1 Buckling Analysis

According to equation (5) the strain variation at the critical point (ϵ_c) can be written as

$$(23) \quad \delta\epsilon_c = L_1(\delta\mathbf{u}) + L_{11}(\mathbf{u}_c, \delta\mathbf{u})$$

Insertion of equations (8) and (9) into equation (10) together with equation (23) gives

$$(24) \quad \mathbf{H}[L_1(\mathbf{u}_1) + L_{11}(\mathbf{u}_c, \mathbf{u}_1)].[L_1(\delta\mathbf{u}) + L_{11}(\mathbf{u}_c, \delta\mathbf{u})] + \sigma_c.L_{11}(\mathbf{u}_1, \delta\mathbf{u}) = 0$$

After some algebraic manipulation on equation (24) and replacing L_1 and L_{11} functionals with the finite element matrices \mathbf{B}_L and \mathbf{B}_{NL} we get the discretized form of equation (24)

$$(25) \quad \delta\mathbf{q}^T[\mathbf{B}_L^T\mathbf{H}\mathbf{B}_L\mathbf{q}_1 + \mathbf{B}_{NL}^T(\mathbf{q}_c)\mathbf{H}\mathbf{B}_L\mathbf{q}_1 + \mathbf{B}_L^T\mathbf{H}\mathbf{B}_{NL}(\mathbf{q}_c)\mathbf{q}_1 + \mathbf{B}_{NL}^T(\mathbf{q}_1)\sigma_c] = 0$$

Because $\delta\mathbf{q}$ is an arbitrary displacement vector we can drop it and rewrite equation (25) after element level integration and assembly process as

$$(26) \quad [\mathbf{K}_M + \mathbf{K}_D(\mathbf{q}_c) + \mathbf{K}_G(\sigma_c)]\mathbf{q}_1 = 0$$

where \mathbf{K}_M , $\mathbf{K}_D(\mathbf{u}_c)$ and $\mathbf{K}_G(\sigma_c)$ are the material, initial displacement and geometric stiffness matrices respectively. They are defined at the element level as

$$\mathbf{K}_M = \int_v \mathbf{B}_L^T\mathbf{H}\mathbf{B}_L dv$$

$$\mathbf{K}_D(\mathbf{q}_c) = \int_v [\mathbf{B}_{NL}^T(\mathbf{q}_c)\mathbf{H}\mathbf{B}_L + \mathbf{B}_L^T\mathbf{H}\mathbf{B}_{NL}(\mathbf{q}_c)] dv$$

$$\mathbf{K}_G(\sigma_c) = \int_v [\sigma_{xxc}\mathbf{K}_{xx} + \sigma_{yy_c}\mathbf{K}_{yy} + \sigma_{zzc}\mathbf{K}_{zz} + \sigma_{xy_c}\mathbf{K}_{xy} + \sigma_{yz_c}\mathbf{K}_{yz} + \sigma_{zx_c}\mathbf{K}_{zx}] dv$$

where v is the element volume, σ_{xxc} , σ_{yy_c} , σ_{zzc} , σ_{xy_c} , σ_{yz_c} , σ_{zx_c} are the stress components and \mathbf{K}_{xx} , \mathbf{K}_{yy} , \mathbf{K}_{zz} , \mathbf{K}_{xy} , \mathbf{K}_{yz} , \mathbf{K}_{zx} have already been defined in equation (22). Now the sum of \mathbf{K}_M , $\mathbf{K}_D(\mathbf{u}_c)$ and \mathbf{K}_G gives the tangent stiffness matrix (\mathbf{K}_{tc}) at the critical point. Therefore equation (26) for the buckling problem can be written as

$$(27) \quad \mathbf{K}_{tc}\mathbf{q}_1 = 0$$

In order to solve equation (27) we can proceed in the following way. First we perform a standard nonlinear analysis to reach as close as possible to the critical point without encountering any negative diagonal term in the system stiffness matrix. Let us define that state as the base state which occurs at $\lambda = \lambda_b$ with the corresponding displacement and stress states \mathbf{q}_b and σ_b respectively. We can now linearize $\mathbf{q}(\lambda)$ and $\sigma(\lambda)$ as

$$(28) \quad \begin{aligned} \mathbf{q}(\lambda) &= \mathbf{q}_b + (\lambda - \lambda_b)\dot{\mathbf{q}}_b \\ \sigma(\lambda) &= \sigma_b + (\lambda - \lambda_b)\dot{\sigma}_b \end{aligned}$$

where dots denote derivatives with respect to λ . At $\lambda = \lambda_c$ equation (28) becomes

$$(29) \quad \begin{aligned} \mathbf{q}(\lambda_c) &= \mathbf{q}_c = \mathbf{q}_b + (\lambda_c - \lambda_b)\dot{\mathbf{q}}_b \\ \sigma(\lambda_c) &= \sigma_c = \sigma_b + (\lambda_c - \lambda_b)\dot{\sigma}_b \end{aligned}$$

Insertion of equation (29) into equation (26) gives

$$(30) \quad \begin{aligned} &[[\mathbf{K}_M + \mathbf{K}_D(\mathbf{q}_b) + \mathbf{K}_G(\sigma_b)] \\ &+ (\lambda_c - \lambda_b)[\mathbf{K}_D(\dot{\mathbf{q}}_b) + \mathbf{K}_G(\dot{\sigma}_b)]]\mathbf{q}_1 = 0 \end{aligned}$$

We can write equation (30) in a concise form using tangent stiffness matrix at the base state (\mathbf{K}_{tb}) as

$$(31) \quad [\mathbf{K}_{tb} + (\lambda_c - \lambda_b)[\mathbf{K}_D(\dot{\mathbf{q}}_b) + \mathbf{K}_G(\dot{\sigma}_b)]]\mathbf{q}_1 = 0$$

Equation (31) is the linear eigenvalue problem for the buckling load λ_c and the buckling mode \mathbf{q}_1 . For the determination of $\dot{\mathbf{q}}_b$ one can proceed considering proportional loading ($\mathbf{f} = \lambda\mathbf{f}_0$) as

$$(32) \quad \dot{\mathbf{q}}_b = \left(\frac{d\mathbf{q}}{d\lambda}\right)_b = \left(\frac{d\mathbf{q}}{d\mathbf{f}}\right)_b \frac{d\mathbf{f}}{d\lambda} = \left(\frac{d\mathbf{q}}{d\mathbf{f}}\right)_b^{-1} \mathbf{f}_0$$

Since $\left(\frac{d\mathbf{f}}{d\mathbf{q}}\right)_b = \mathbf{K}_{tb}$ equation (32) can be rewritten as

$$(33) \quad \dot{\mathbf{q}}_b = \mathbf{K}_{tb}^{-1}\mathbf{f}_0$$

Therefore $\dot{\mathbf{q}}_b$ can be obtained from the linear solution of

$$(34) \quad \mathbf{K}_{tb}\dot{\mathbf{q}}_b = \mathbf{f}_0$$

3.2 Post-buckling Analysis

Insertion of equations (8), (9), (13), (14) and (23) into equation (15) and some algebraic manipulations finally give

$$(35) \quad \begin{aligned} &\mathbf{H}[L_1(\mathbf{u}_2) + L_{11}(\mathbf{u}_c, \mathbf{u}_2)].[L_1(\delta\mathbf{u}) \\ &+ L_{11}(\mathbf{u}_c, \delta\mathbf{u})] + \sigma_c.L_{11}(\mathbf{u}_2, \delta\mathbf{u}) = \\ &-\frac{1}{2}\mathbf{H}[L_2(\mathbf{u}_1)].[L_1(\delta\mathbf{u}) + L_{11}(\mathbf{u}_c, \delta\mathbf{u})] \\ &- \mathbf{H}[L_1(\mathbf{u}_1) + L_{11}(\mathbf{u}_1, \mathbf{u}_c)].L_{11}(\mathbf{u}_1, \delta\mathbf{u}) \end{aligned}$$

In terms of finite element matrices equation (35) can be written as

$$(36) \quad \begin{aligned} & \delta \mathbf{q}^T [\mathbf{B}_L^T \mathbf{H} \mathbf{B}_L \mathbf{q}_2 + \mathbf{B}_{NL}^T(\mathbf{q}_c) \mathbf{H} \mathbf{B}_L \mathbf{q}_2 \\ & + \mathbf{B}_L^T \mathbf{H} \mathbf{B}_{NL}(\mathbf{q}_c) \mathbf{q}_2 + \mathbf{B}_{NL}^T(\mathbf{q}_2) \boldsymbol{\sigma}_c] = \\ & - \delta \mathbf{q}^T \left[\frac{1}{2} [\mathbf{B}_L + \mathbf{B}_{NL}(\mathbf{q}_c)]^T \mathbf{H} \mathbf{B}_{NL}(\mathbf{q}_1) \mathbf{q}_1 \right. \\ & \left. + \mathbf{B}_{NL}^T(\mathbf{q}_1) \mathbf{H} [\mathbf{B}_L + \mathbf{B}_{NL}(\mathbf{q}_c)] \mathbf{q}_1 \right] \end{aligned}$$

We notice that the left hand side of equation is identical to that of equation (25) with the only difference that \mathbf{q}_2 appears in place of \mathbf{q}_1 . Further we identify the right hand side of equation as a force vector denoted by \mathbf{g} . Under these considerations we can write equation (36) in a compact form as

$$(37) \quad [\mathbf{K}_{tb} + (\lambda_c - \lambda_b) [\mathbf{K}_D(\dot{\mathbf{q}}_b) + \mathbf{K}_G(\dot{\boldsymbol{\sigma}}_b)]] \mathbf{q}_2 = \mathbf{g}$$

where we assume the same linearization as defined in equation (28). Because equation (37) is singular we introduce a factor $\alpha < 1$ and rewrite equation as

$$(38) \quad [\mathbf{K}_{tb} + \alpha(\lambda_c - \lambda_b) [\mathbf{K}_D(\dot{\mathbf{q}}_b) + \mathbf{K}_G(\dot{\boldsymbol{\sigma}}_b)]] \mathbf{q}_2 = \mathbf{g}$$

Solution of equation (38) gives the second order modes \mathbf{q}_2 . The associated orthogonality constraint as defined by equation (16) can be translated to finite element context as

$$(39) \quad \mathbf{q}_1^T \mathbf{K}_G(\boldsymbol{\sigma}_c) \mathbf{q}_2 = 0$$

In order to determine the b coefficient as defined by equation (17) one needs to compute \mathbf{q}_1 , \mathbf{q}_2 , \mathbf{q}_c and $\dot{\mathbf{q}}_c$. In subsections (3.1) and (3.2) we discussed about the determination process of \mathbf{q}_1 , \mathbf{q}_2 , \mathbf{q}_c . Since we made the base state (at $\lambda = \lambda_b$) very close to the critical state we can assume

$$(40) \quad \begin{aligned} \dot{\mathbf{q}}_c & \approx \dot{\mathbf{q}}_b \\ \dot{\boldsymbol{\sigma}}_c & \approx \dot{\boldsymbol{\sigma}}_b \end{aligned}$$

Solution of equation (34) gives $\dot{\mathbf{q}}_b$ and consequently $\dot{\boldsymbol{\sigma}}_b$.

4 NUMERICAL EXAMPLES

In order to verify the correctness of the approach we will consider a reference isotropic conical shell representative of the conical interstage of the Vega Launcher structure. The conical shell is loaded under axial compression. One end of the conical shell is fixed and an axial load is applied at the other end. In order to apply simply supported boundary condition all the displacement degrees of freedoms are restrained at the edge of the fixed end while the rotational degrees of freedoms remain free. At the loaded end the displacements in the plane of the edge are restrained but the axial displacements are set free

so that the load can be applied. However we constrain those axial displacements such that they remain the same at all nodes of the edge and thereby eliminating the possibility of warping at the edge. This boundary condition is known as MSS4 [13]. The dimensions of the reference conical shell are:

Top radius R_1 : 937 mm
Bottom radius R_2 : 1489.5 mm
Height H : 2138 mm

Apart from the reference shell we will also consider a few other shells generated by varying the height H , the thickness t and the semi vertex angle α of the reference shell keeping the top radius R_1 unchanged. For the case with $\alpha = 0$ the reference conical shell indeed becomes a cylindrical shell. For the cylindrical shell we will use two different types of simply supported boundary conditions known as SS-3 and SS-4 [13]. In case of SS-3 warping at the edges are allowed while for SS-4 it is not allowed. In fact SS-4 is equivalent to MSS4 (applicable for conical shells).

In table 1 the results obtained for the reference conical shell and two other conical shells with half height (height = $0.5H$) and double thickness (thickness = $2t$) of the reference shell are given under MSS4 boundary condition. Table 2 shows the results for the cylindrical shell generated by setting the semi vertex angle to zero ($\alpha = 0$) of the reference shell under both MSS4 and SS3-Schiffner boundary conditions. The first buckling loads and b coefficients are compared between DIANA and the semi-analytical tools BAAC [13] (for conical shells) and ANILISA [8, 9] (for cylindrical shells) which are based on Donnell's shell theory. In the second column of both of the tables 'N' indicates the number of circumferential full waves appearing in the first buckling mode. In the third column 'Mesh' indicates the mesh size in terms of the number of divisions around the circumference times the number of divisions along the length. The buckling modes are scaled such that the maximum radial displacement is equal to the shell thickness.

Figure 1 shows the pre-buckling displacement field of the reference conical shell at the base state when $\lambda = \lambda_b$. Figures 2 and 3 show the first buckling (\mathbf{q}_1) mode and the corresponding second order mode (\mathbf{q}_2) respectively. The buckling mode consists of 10 circumferential full waves and does not contain any axisymmetric component. The second order mode contains twice the number of circumferential full waves of the buckling mode. In addition an axisymmetric contraction is also present. These displacement modes show the same shape as predicted

by the semi-analytical approach.

5 CONCLUSIONS

A finite element implementation of Koiter's initial post-buckling theory including the effect of pre-buckling nonlinearity has been presented. This work is an extension of the existing implementation in DIANA and a similar implementation in MATLAB done by Tiso [11]. In those implementations a linear pre-buckling state was assumed. In this work we dealt with axially loaded conical and cylindrical shells where the effect of pre-buckling nonlinearity is high and in these cases it is not always possible to capture the first buckling mode with the assumption of the linear pre-buckling state. Also the additional terms triggered by the pre-buckling nonlinearity in the calculation of the second order modes and the b coefficients are no longer negligible. Therefore the effect of pre-buckling nonlinearity has been included in the present implementation. The obtained buckling modes and loads along with the corresponding second order modes and b coefficients were in reasonable agreement with those predicted by the semi-analytical approach. The small discrepancies in buckling loads and b coefficients are probably due to the approximation of the Donnell's theory used in the semi-analytical approach as compared to the kinematic model used in the present approach (see section 3).

This implementation has been done for a single mode analysis (only the first buckling mode has been considered). It can be further extended for a multi mode analysis. Also geometric imperfections can be included in the perturbation expansion in order to estimate the reduction of the load carrying capacity.

ACKNOWLEDGEMENT

This research is supported by the Dutch Technology Foundation STW, applied science division of NWO and the Technology Program of the Ministry of Economic Affairs (STW project DLR.6613).

References

[1] J. W. Hutchinson E. Byskov. Mode interaction in axially stiffened cylindrical shells. *AIAA Journal*, 15:941–948, 1977.

[2] P. Tiso, E. L. Jansen, and M. M. Abdalla. A reduction method for finite element nonlinear dynamic analysis of shells. In *RA Naik (Ed.), 47th AIAA/ASME/ASCE/AHS/ASC Structures, Structural Dynamics and Materials Conference*. Reston, VA: AIAA, pages 1–13, 2006.

[3] T. J. A. M. Hermens, E. L. Jansen, and P. Tiso. A finite element based perturbation method for vibrations of imperfect structures. In *Proceedings of the European Conference of Spacecraft Structures, Materials and Mechanical Testing, Noordwijk, The Netherlands*, pages 1–8, 2005.

[4] W. T. Koiter. *On the stability of the elastic equilibrium*. PhD thesis, Delft University of Technology (in Dutch), 1945.

[5] Vega - the small launcher for europe. Technical Report ESA BR-257, European Space Agency, 2005.

[6] G. A. Cohen. Effect of a nonlinear prebuckling state on the postbuckling behavior and imperfection sensitivity of elastic structures. *AIAA Journal*, 6:1616–1619, 1968.

[7] J. R. Fitch. The buckling and postbuckling behavior of spherical caps under concentrated loads. *International Journal of Solids and Structures*, 4:421–446, 1968.

[8] J. Arbocz and J. M. A. M. Hol. Koiter's stability theory in a computer-aided engineering (cae) environment. *International Journal of Solids Structures*, 26:945–975, 1990.

[9] J. Arbocz and J. M. A. M. Hol. Anilisa - computational module for koiter's imperfection sensitivity theory. Technical Report LR-582, Delft University of Technology, 1989.

[10] *DIANA User's Manual - Release 9.2*. Delft, The Netherlands, 2007.

[11] P. Tiso, M. M. Abdalla, and E. L. Jansen. Koiters' post-buckling analysis of general shell structures using the finite element method. In *Proceedings of the 25th international congress of the aeronautical sciences, Hamburg, Germany: ICAS*, pages 1–13, 2006.

[12] B. Budiansky. Dynamic buckling of elastic structures: criteria and estimates. In *Dynamic Stability of Structures*. Pergamon Press, 1965. Proceedings of International Conference, Northwestern University, Evanston, Illinois.

[13] G. Zhang. *Stability Analysis of Anisotropic Conical Shells*. PhD thesis, Delft University of Technology, 1993.

| Geometric parameters | N | Mesh | Buckling load [N] | | <i>b</i> coefficient | |
|----------------------|----|----------|----------------------|-----------------------|----------------------|----------|
| | | | BAAC | DIANA | BAAC | DIANA |
| Reference | 10 | 120 × 36 | 9.1071×10^6 | 8.98950×10^6 | -0.44032 | -0.46870 |
| Height = $0.5H$ | 10 | 196 × 32 | 9.0649×10^6 | 8.9583×10^6 | -0.38626 | -0.39691 |
| Thickness = $2t$ | 7 | 120 × 36 | 3.6412×10^7 | 3.5649×10^7 | -0.42213 | -0.41319 |

Table 1: Comparison of buckling load and *b* coefficients of conical shells

| Boundary condition | N | Mesh | Buckling load [N] | | <i>b</i> coefficient | |
|--------------------|----|----------|----------------------|---------------------|----------------------|----------|
| | | | ANILISA | DIANA | ANILISA | DIANA |
| SS-4 | 10 | 120 × 44 | 9.7523×10^6 | 9.645×10^6 | -0.45467 | -0.43667 |
| SS-3 | 10 | 120 × 44 | 9.4996×10^6 | 9.379×10^6 | -0.51188 | -0.50208 |

Table 2: Comparison of buckling load and *b* coefficients of cylindrical shells

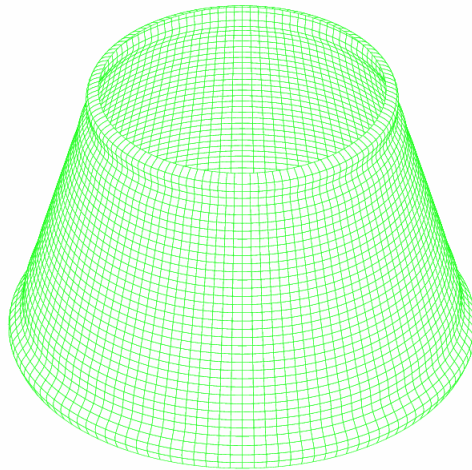


Figure 1: The pre-buckling mode

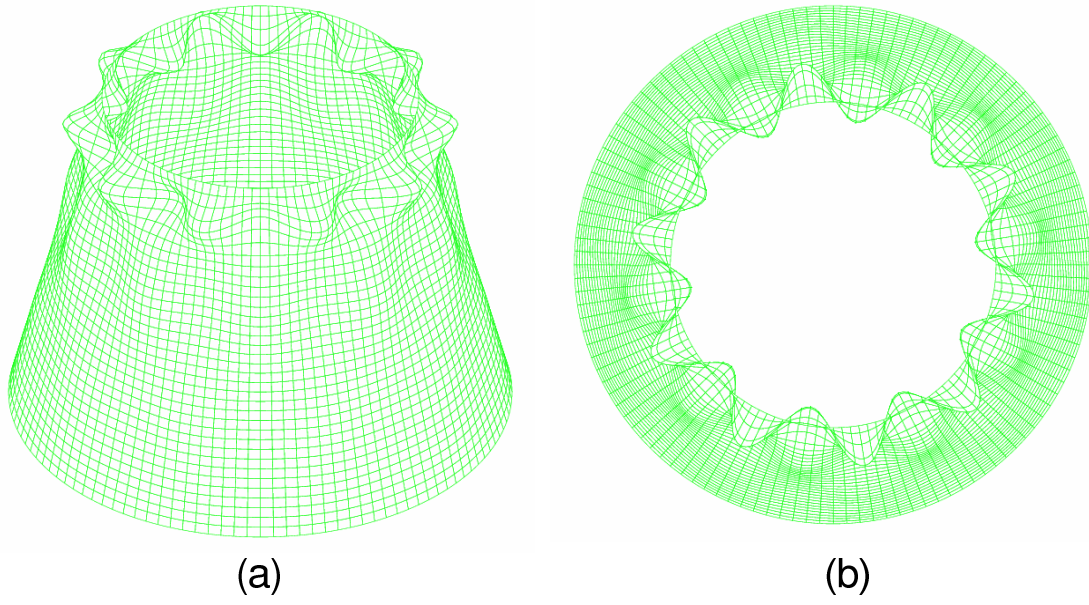


Figure 2: The first buckling mode: (a) Isometric view (b) Top view

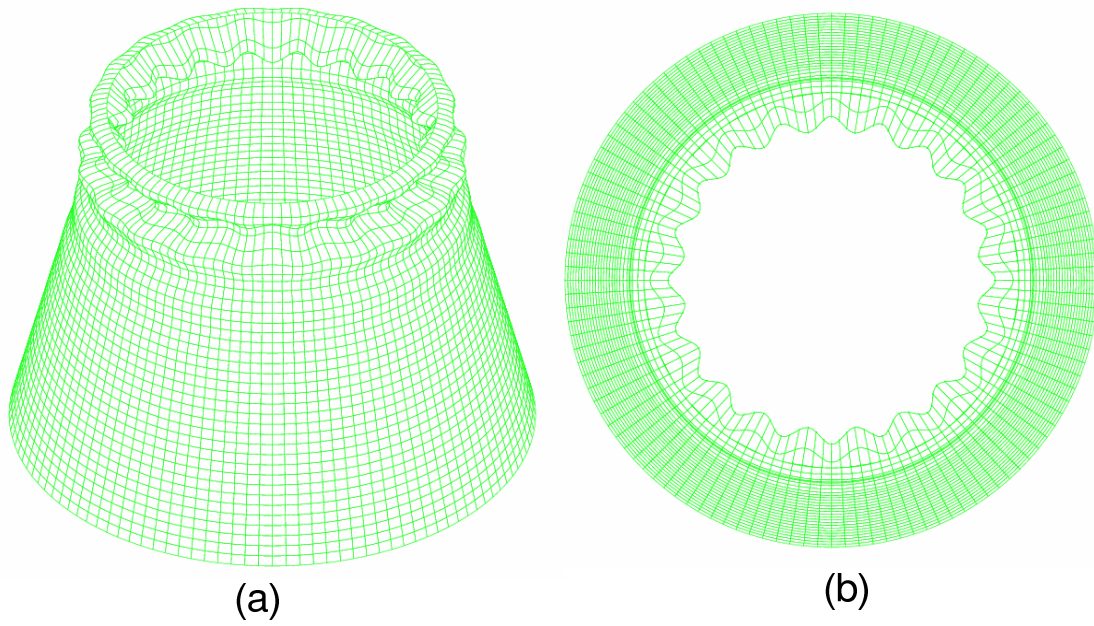


Figure 3: The second order mode: (a) Isometric view (b) Bottom view